Preparation of Sulfapyridine Prodrugs and their Nanoscale Self-assemblies for the Management of Rheumatoid Arthritis

1. Introduction

Rheumatoid arthritis (RA), the most prevalent systemic inflammatory disease, that not only affects the joints, but also includes extra-articular manifestations, therefore must be regarded as syndrome [1]. In the past three decades, therapeutic resources for the management of RA have grown tremendously, which include disease modifying anti-rheumatic drugs i.e., DMARDs, both of synthetic and of biological origin, non-steroidal anti-inflammatory drugs (NSAIDs), and glucocorticoids [2]. Despite of extensive research, management of RA is still challenging because of unfavorable properties of existing medications such as instability, poor aqueous solubility, low cell permeability, and rapid metabolism, all contributing towards the low bioavailability of drug at the target site, thereby require frequent administration and may lead to toxicity [3].

Novel drug delivery system is an excellent strategy to improve pharmacokinetic properties of various drugs with diverse physiochemical properties [4, 5]. Among the various delivery systems explored, the major cluster of research has been accomplished through the use of drug nanocarriers *e.g.* hydrogels [6], liposomes [7], dendrimers [8] and polymeric nanoparticles/nanospheres/nanocapsules [9]. These delivery systems not only shield the cargo drug, but also effectively transport molecules to the targeted sites, leading to improvement of bioavailability and efficacy, in addition to solubility and stability [10]. However inefficient drug loading/releasing pattern and biosafety issues of these delivery systems still remain a challenging task [11]. A prodrug based self-assembled nanostructures that spontaneously form supramolecular structures in aqueous media via hydrophilic and hydrophobic interactions have opened up new avenues in targeted drug delivery. The nanoscale structure provides protection to the drug during storage and administration, and fulfill the strategic role that excipient play in conventional drug development process [12]. With enormous advantages, self-assembling prodrugs exhibit high drug loading capacity, passive targeting ability, prevent premature leakage, reduce renal clearance, extends circulation half-life and improved cellular uptake [13].

Recently, stimuli-responsive nanoplatforms triggered by endogenous (such as pH, ROS, GSH, enzymatic, etc.) or exogenous (such as magnetic fields, light, electric pulses, etc.) stimuli have been developed for targeted delivery of drugs[14]. The synovial fluid of rheumatic patients contains elevated levels of a series of enzymes including matrix metalloproteinases (MMPs), cysteine protease, and hyaluronidase [15]. Moreover, an increased level of reactive oxygen species in RA patients as a result of a hypoxic and inflammatory situation [16], and weakly acidic microenvironment (pH less than 6) [17] can be used as trigger to release the drug from nanoparticles at the target side for sustained action. Based on the above hypothesis, we propose to give a second life to the long-abandoned drug, SP, which, due to its high toxicity index could not be explored for anti-inflammatory potential [4]. In the present research, we have synthesized various amphiphilic prodrugs of SP by conjugating with a pro-moieties via enzyme- and acid-sensitive amide bond, which formed self-assembled nanostructures in aqueous environment. Single intra-articular injection of self-assembled nanostructures of SP

prodrug successfully mitigated adjuvant-induced inflammatory arthritis in rats, indicating the prolonged retention of nanoparticles in the arthritic joints by virtue of their size as well as two-step release of the entrapped drug i.e., disassembly and followed by lysis of prodrug to release the active drug. The present research is expected to provide a prolonged, sustained, economical and patient-friendly treatment option in the management of arthritis. The summary of the research work has been depicted in Figure 1.

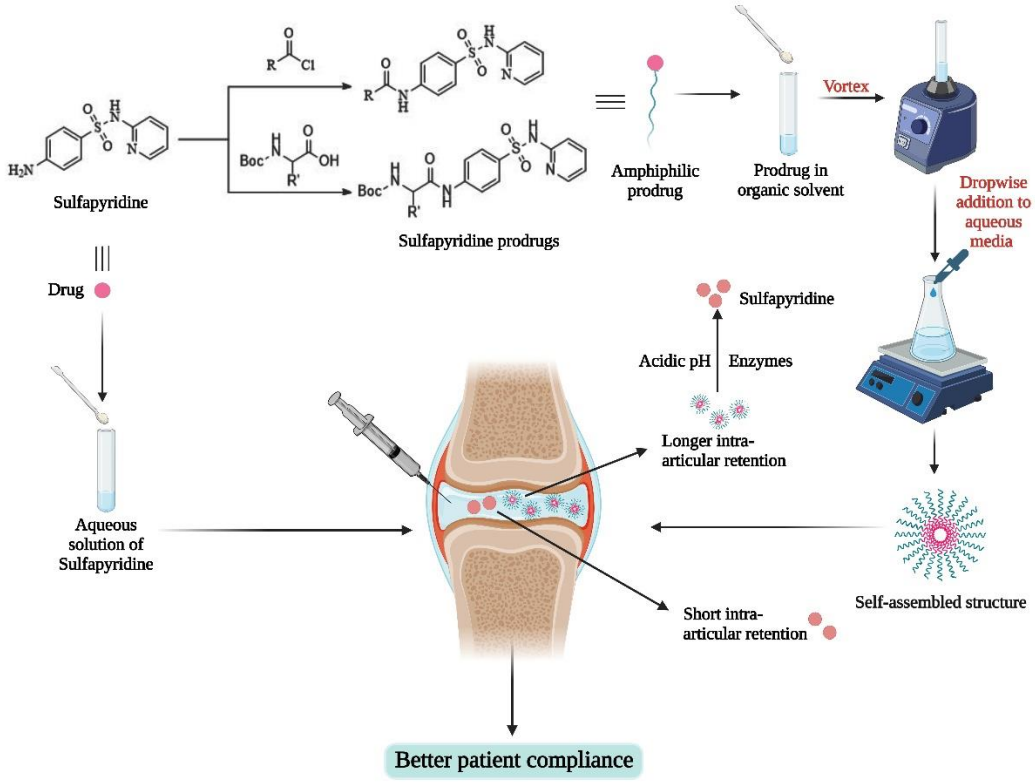

Figure 1: Rationale of better therapeutic efficacy of self-assembled nanostructures of amphiphilic prodrugs

2. Objectives

- Synthesis and characterization of amide prodrugs of sulfapyridine
- Analytical method development of sulfapyridine and its prodrugs
- Thermodynamic equilibrium solubility studies and partition coefficient
- Assessment and characterization of prodrugs for self-assembly in aqueous solutions
- *In vivo* anti-arthritic activity of supramolecular prodrugs in rats

3. Materials and methods

3.1 Materials

Sulfapyridine (>99%), Boc-glycine, Boc-L-Alanine, Boc-L-Leucine, Boc-L-Proline, Complete Freund's Adjuvant (CFA), were purchased from Sigma-Aldrich (St. Louis, MO, USA). Hyaluronic acid was provided by Alpha chem. Pvt. Ltd. (India). Dimethyl formamide was obtained from Rankem (India). Ketamine was purchased from Aneket (Neon labs Ltd., India). HPLC grade acetonitrile was obtained from Loba Chemie Pvt. Ltd. (India). Ethyl acetate and sodium hydroxide were provided by Molychem (India). *n*-octanol was purchased from central

drug house Pvt. Ltd. (New Delhi, India). Purified water was obtained from Bio-Age water system (India). Propionyl chloride, valeryl chloride, pivaloyl chloride, hexanoyl chloride, heptanoyl chloride, octanoyl chloride, nonanoyl chloride, decanoyl chloride, undecanoyl chloride, dodecanoyl chloride, stearoyl chloride, 4-pentenoyl chloride, oleoyl chloride, 10-undecenoyl chloride, silica gel 100-200 mesh, cholesterol, citric acid, formalin, formic acid, ortho phosphoric acid, hydrochloric acid, calcium chloride, methanol, ethanol, chloroform, disodium hydrogen phosphate, potassium carbonate, potassium chloride, potassium dihydrogen phosphate, and sodium chloride were provided by Loba Chemie Pvt. Ltd. (India). Thin layer chromatography (TLC) plate was provided by Merck KGaA (Darmstadt, (Germany). Rat IL-6 and TNF-α ELISA kits were purchased from RayBiotech (USA).

3.2 Animals

Male Wistar albino rats (n = 36; age, 7-8 weeks; weight, 150-200 g) were purchased from the animal house of Lovely Professional University (Jalandhar, India). The animals were housed in clean polypropylene cages and had free access to food and water. Clean sterilized paddy husk was given as a bedding material. The room temperature was maintained at 23-25^{o}C, with relative humidity 50-60% as well as 12h of light/dark cycle as per Committee for Control and Supervision of Experiments on Animals (CCSEA) guidelines. All the described animal protocols and experiments were reviewed and approved by the Institutional Animal Ethics Committee, Lovely Professional University, Jalandhar (approval no. LPU/IAEC/2023/49) before performing the experiment.

3.3 Equipments

Infrared (IR) spectra were recorded on a Shimadzu FTIR 8400S spectrophotometer. ^{1}H and ^{13}C nuclear magnetic resonance (NMR) were acquired on a Bruker Avance-II (400 MHz) spectrometer in dimethyl sulfoxide-d6 (DMSO) using tetramethylsilane as internal reference. Mass spectra was recorded on a Maldi Synapt XS HD mass spectrometer using electron spray ionization (ESI). The UV absorption maxima (λ_{max}) of the prodrug was carried out on a UV spectrophotometer (Shimadzu UV-1800, AX200, Japan). Thermal analysis was carried out with the DSC Q200 machine from TA instruments. The samples were quantified using an HPLC system (Shimadzu LC-20AD Prominence). The mean size and zeta potential of formulations were determined using a Zeta sizer Nano ZS90 instrument (Malvern, UK). Joint diameter of male Wistar Albino rats was measured by using a digital vernier calliper (Mitutoyo, Mumbai), and paw volume was measured by the Plethysmometer VJDP-01 (Washim, India)

3.4 Methods

3.4.1 Synthesis of *N*-substituted fatty acid-based SP prodrugs

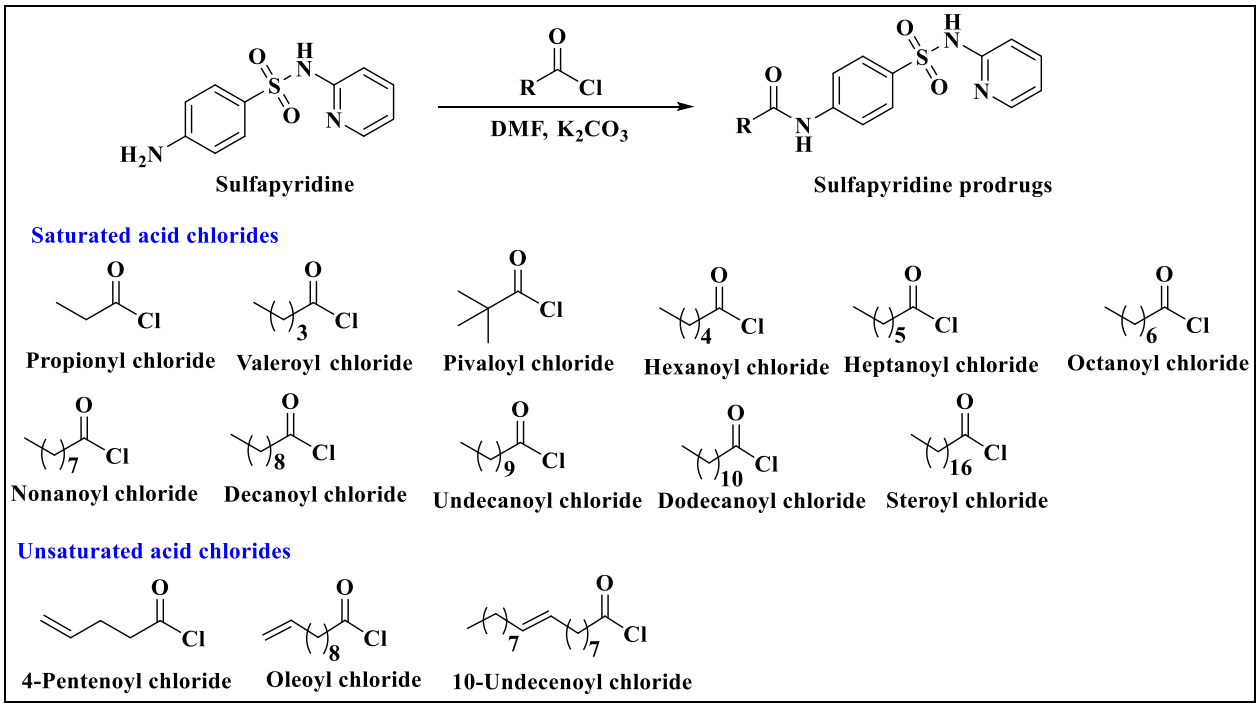

Figure 2: General scheme for the synthesis of *N*-substituted fatty acid prodrugs

SP (0.002 mole) was dissolved in anhydrous dimethyl formamide (DMF) (2 mL) and potassium carbonate (K_2CO_3) (0.006 mole) was added to the solution. The flask was kept on magnetic stirrer and respective acid chloride (0.004 mole) was added to the drug solution drop-wise while the solution was being stirred continuously. During the addition, the temperature of the flask was maintained at 15-20℃ by keeping the solution under ice bath. After addition of acid chloride, the flask was closed with calcium chloride guard tube and the reaction mixture was stirred at room temperature till the completion of the reaction. The desired compound was purified by column chromatography using chloroform-methanol as mobile phase.

3.4.2 Synthesis of *N*-substituted amino acid-based prodrugs of SP

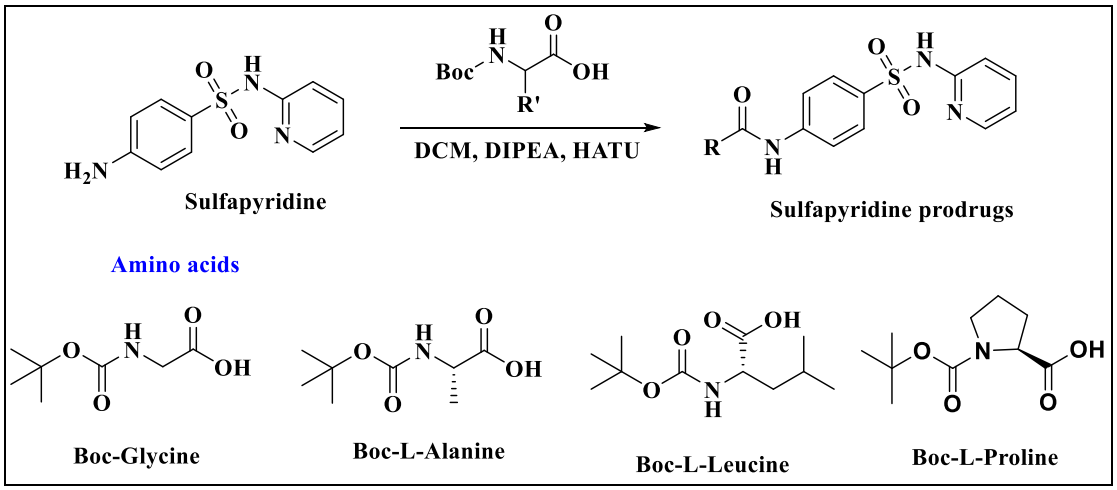

Figure 3: General scheme for the synthesis of *N*-substituted amino acid-based prodrugs of SP

To the solution of Boc-protected L-amino acid (0.001 mole) in dichloromethane (DCM) (2 mL), SP (0.001 mole), *N*,*N*-Diisopropylethylamine (DIPEA) (0.003 mole) and hexafluorophosphate azabenzotriazole tetramethyl uronium (HATU) (0.0015 mole) were added. Thereafter, the reaction mixture was stirred under anhydrous conditions at room temperature till the completion of the reaction. After completion of the reaction, water (10 mL) was added to the reaction mixture, and the prodrug was extracted with ethyl acetate. The combined organic layer was washed with 2N HCl. The synthesized prodrug was purified by column chromatography.

3.4.3 Characterization of Prodrugs

The synthesized molecules were characterized by IR, NMR and Mass spectral analysis. The precise melting point of organic samples were determined by DSC, while the purity was determined by HPLC.

3.4.4 Fabrication and characterization of Self-assembled nanostructures

Prodrugs were dissolved in organic solvent and then rapidly injected into water to observe their solubility. The solution was further dialyzed using water to remove organic solvent. The morphology and hydrodynamic diameters of self-assembled nanostructures were investigated by microscopy and dynamic light scattering particle size analyzer respectively.

3.4.5. Analytical method development and validation

HPLC Shimadzu LC20AD, fitted with quaternary solvent manager, binary pump, online degasser, and photodiode array (PDA) detector was used for the method development and validation. The analysis of SP prodrug was carried out at an ambient temperature using reverse phase Nucleodur® C18 (250 x 4.6 mm, 5 µm) column. The mobile phase consisted of 0.1% v/v formic acid (35%) and acetonitrile (65%). The mobile phase was filtered through 0.22 µm nylon membrane filter and delivered at a constant flow rate of 1 mL/min. The injection volume was 25 µL and the analytes were detected by UV at 265 nm. The method was validated for Accuracy, Precision (Repeatability and Intermediate Precision), Specificity, Detection limit, Quantitation limit, Linearity, and Range as per ICH Q2 (R1) guidelines and the respective chromatogram.

3.4.6 Determination of Equilibrium solubility and partition coefficient

Equilibrium solubility and partition coefficient of the synthesized prodrugs as well as of SP were determined by shake-flask experiments.

Briefly, an excess of compound was added to vials containing 5 ml of solvent or simulated synovial fluid (SSF). The solution containing solid excess of the sample was then capped, and stirred at 37 ± 1°C temperature for 24 h. The equilibrated samples were centrifuged at 8000 rpm for 10 minutes at 37 ± 1°C in order to remove the undissolved drug. The clear supernatant was taken out with a fine pipette from the saturated solution, filtered through 0.22 µ filter and diluted with solvent (maintained at 37 ± 1°C), if necessary. The concentration of drug in each aliquot was measured by HPLC.

Partition coefficients of SP and prodrugs was determined using *n*-octanol and SSF. The two phases of the liquid system were well saturated with each other for 24 h on a mechanical shaker before use. These pre-saturated solvents were used to determine the partition coefficient of the compounds. A known quantity of sample was added to 20 mL of pre-saturated *n*-octanol and SSF mixture and kept on mechanical shaker at 37 ± 1°C for 24 h and 100 rpm. The flask was kept undisturbed for 2 h for complete separation of both the phases and drug content in both organic and aqueous phase was determined by HPLC after suitable dilution.

3.4.7 *In vitro* cytotoxicity studies

The *in vitro* cytotoxicity of SP and its prodrug was evaluated by MTT assay using L929 cell line (Mouse Fibroblast cell line).

3.4.8 *In vivo* anti-arthritic activity

The anti-arthritic activity of self-assembled nanoparticles was evaluated in rats using complete Freund's adjuvant-induced arthritis model. Anti-arthritic potential of treatment groups was evaluated based on various parameters such as paw volume, joint diameter, and body weight on day 0 and thereafter every fourth day till day 28. On day 28, blood was withdrawn by retro-orbital puncture and used for estimation of various biochemical parameters (serum aspartate aminotransferase, alanine aminotransferase, alkaline phosphatase, and total protein levels), hematological parameters (RBC count, WBC count, Hb, platelets, ESR and serum RF) and serum inflammatory mediators such as TNFα and IL-6. Radiographs of joints of hind paws of rats was taken using X-ray tube assembly.

4. Results

4.1 Characterization of amide prodrugs of SP

N-(4-(N-(pyridin-2-yl)sulfamoyl)phenyl)propionamide (SP-PROP)

Cream white powder; Yield: 30%; UV absorption maxima:265nm; m.p. (DSC) 213.89°C; ^{1}H NMR (400 MHz, DMSO) δ 10.23 (s, 1H, amide-H), 8.00 (d, *J* = 4.6 Hz, 1H, Ar-H), 7.86 – 7.59 (m, 5H, Ar-H), 7.12 (d, *J* = 8.6 Hz, 1H, Ar-H), 6.96 – 6.72 (m, 1H, Ar-H), 2.33 (q, *J* = 7.5 Hz, 2H, CH_2), 1.06 (t, *J* = 7.5 Hz, 3H, CH_3); ^{13}C NMR (500 MHz, DMSO): 172.48, 152.75, 143.88, 142.61, 139.84, 135.07, 127.68, 118.30, 115.78, 113.29, 29.46, 9.32; IR (KBr) ν: 3321 (N-H str. SO_2NH/CONH), 2924 (C-H str. Ar-H), 2811 (C-H str. aliphatic), 1670 (C=O str. amide), 1629 and 1460 (C=C ArH), 1597 (N-H bending CONH), 1531 (N-H bending SO_2NH), 1384 (S=O asymm. str.), 1280 (C-N str.), 1135 (S=O symm. str.), 833 (para oop), 786 (S-N str.); Mass (m/z): 306.15 ($M+H^+$); HPLC purity: 97.92%

N-(4-(N-(pyridin-2-yl)sulfamoyl)phenyl)pentanamide (SP-VAL)

Cream white powder; Yield: 28.44%; UV absorption maxima:265nm; m.p.(DSC) 187.83°C ; ^{1}H NMR (400 MHz, DMSO) δ 10.22 (s, 1H, amide-H), 8.01 (d, *J*= 4.4 Hz, 1H,Ar-H), 7.76 (m, 5H,Ar-H), 7.12 (d, *J* = 8.4 Hz, 1H, Ar-H), 7.00 – 6.79 (m, 1H, Ar-H), 2.34 (t, *J* = 7.2 Hz,

2H,CH_2), 1.66 –1.51 (m, 2H, CH_2), 1.31 (m, 2H, CH_2), 0.88 (t, *J* = 7.2 Hz, 3H, CH_3). ^{13}C NMR (500 MHz, DMSO): 171.77, 152.74, 143.98, 142.57, 139.83, 135.11, 127.67, 116.32, 115.84, 113.27, 36.04, 26.95, 21.64, 13.57; IR (KBr) ν: 3298 (N-H str. SO_2NH/CONH), 2926 (C-H str. ArH), 2858 (C-H str. aliphatic), 1665 (C=O str. amide), 1628 and 1460 (C=C ArH), 1595 (N-H bending CONH), 1532 (N-H bending SO_2NH), 1381 (S=O asymm. str.), 1272 (C-N str.), 1133 (S=O symm. str.), 831 (para oop), 787 (S-N str.); Mass (m/z): 334.25 ($M+H^+$); HPLC purity: 95.52%

N-(4-(N-(pyridin-2-yl)sulfamoyl)phenyl)pivalamide (SP-PIVA)

Cream white powder; Yield: 58.71%; UV absorption maxima:265 nm; m.p. (DSC) 232.80°C; ^{1}H NMR (400 MHz, DMSO) δ 9.52 (s, 1H, amide-H), 7.97 (d, *J* = 24.0 Hz, 1H, Ar-H), 7.80 – 7.54 (m, 5H, Ar-H), 7.12 (d, *J* = 8.6 Hz, 1H, Ar-H), 6.87 (t, *J* = 6.3 Hz, 1H, Ar-H), 1.20 (s, 9H); ^{13}C NMR (500 MHz, DMSO): 176.83, 152.72, 143.98, 142.72, 139.81, 135.25, 127.39, 119.39, 115.88, 113.24, 39.42, 26.87; IR (KBr) ν: 3331 (N-H str. SO_2NH/CONH), 2921 (C-H str. ArH), 2851 (C-H str. aliphatic), 1677 (C=O str. amide), 1629 and 1459 (C=C ArH), 1590 (N-H bending CONH), 1518 (N-H bending SO_2NH), 1383 (S=O asymm. str.), 1278 (C-N str.), 1132 (S=O symm. str.), 999 (para oop), 838 (S-N str.); Mass (m/z): 334.15 ($M+H^+$); HPLC purity: 98.91%

N-(4-(N-(pyridin-2-yl)sulfamoyl)phenyl)hexanamide (SP-HEX)

Cream white powder; Yield: 73%; UV absorption maxima:265nm; m.p. (DSC) 198.96°C ; ^{1}H NMR (400 MHz, DMSO) δ 10.21 (s, 1H,amide-H), 8.02 (d, *J* = 4.4 Hz, 1H, Ar-H), 7.89 – 7.62 (m, 5H, Ar-H), 7.12 (d, *J* = 8.6 Hz, 1H, Ar-H), 6.96 – 6.61 (m, 1H, Ar-H), 2.31 (t, *J* = 7.4 Hz, 2H, CH_2), 1.67 – 1.47 (m, 2H, CH_2), 1.42 – 0.95 (m, 4H, CH_2), 0.86 (t, *J* = 6.9 Hz, 3H,CH_3). ^{13}C NMR (500 MHz, DMSO): 171.79, 152.77, 143.90, 142.60, 139.81, 135.13, 127.70, 118.35, 115.82, 113.28, 36.32, 30.72, 24.52, 21.76, 13.80; IR (KBr) ν: 3320 (N-H str. SO_2NH/CONH), 2927 (C-H str. ArH), 2857 (C-H str. aliphatic), 1668 (C=O str. amide), 1630 and 1461 (C=C ArH), 1596 (N-H bending CONH), 1528 (N-H bending SO_2NH), 1383 (S=O asymm. str.), 1271 (C-N str.), 1136 (S=O symm. str.), 1110 (para oop), 832 (S-N str.); Mass (m/z): 348.30 ($M+H^+$); HPLC purity: 94.07%

N-(4-(N-(pyridin-2-yl)sulfamoyl)phenyl)Heptanamide (SP-HEPT)

Cream white powder; Yield: 34%; UV absorption maxima:265nm; m.p. (DSC) 192.82°C; ^{1}H NMR (400 MHz, DMSO) δ 10.23 (s, 1H,amide-H), 8.02 – 8.03 (d, J = 4.3 Hz, 1H,Ar-H), 7.68 – 7.82 (m, 5H,Ar-H), 7.12 – 7.14 (d, J = 8.6 Hz, 1H,Ar-H), 6.85 – 6.88 (m, 1H,Ar-H), 2.30 – 2.34 (t, J = 7.4 Hz, 2H,CH_2), 1.53-1.58 (m, 2H, CH_2), 1.26 (m, 6H), 0.83 – 0.86 (t, J = 8.9, 4.6 Hz, 3H, CH_3). ^{13}C NMR (500 MHz, DMSO): 171.77, 152.76, 142.55, 139.85, 139.05, 135.15, 127.68, 118.32, 115.79, 113.29, 36.33, 30.88, 28.15, 24.78, 21.84, 13.79; IR (KBr) ν: 3330 (N-H str. SO_2NH/CONH), 2924 (C-H str. ArH), 2858 (C-H str. aliphatic), 1699 (C=O str. amide), 1629 and 1462 (C=C ArH), 1593 (N-H bending CONH), 1523 (N-H bending SO_2NH), 1379 (S=O asymm. str.), 1276 (C-N str.), 1131 (S=O symm. str.), 845 (para oop), 781 (S-N str.); Mass (m/z): 362.5 ($M+H^+$); HPLC purity: 99.47%

N-(4-(N-(pyridin-2-yl)sulfamoyl)phenyl)octanamide (SP-OCT)

Cream white powder; Yield: 89%; UV absorption maxima:265nm; m.p. (DSC) 218.47°C; ^{1}H NMR (400 MHz, DMSO) δ 10.21 (s, 1H, amide-H), 8.02 (d, *J* = 4.4 Hz, 1H, Ar-H), 7.83 – 7.56 (m, 5H, Ar-H), 7.12 (d, *J* = 8.6 Hz, 1H, Ar-H), 7.02 – 6.87 (m, 1H, Ar-H), 2.31 (t, *J* = 7.4 Hz, 2H, CH_2), 1.67 – 1.50 (m, 2H, CH_2), 1.25 (m, 8H), 0.85 (t, *J* = 6.9 Hz, 3H, CH_3).^{13}C NMR (500 MHz, DMSO): 171.76, 152.76, 143.95, 142.56, 139.81, 135.11, 127.68, 118.32, 115.79, 113.26, 36.33, 31.01, 28.44, 28.31, 24.82, 21.92, 13.79; IR (KBr) ν: 3324 (N-H str. SO_2NH/CONH), 2921 (C-H str. ArH), 2851 (C-H str. aliphatic), 1700 (C=O str. amide), 1629 and 1462 (C=C ArH), 1593 (N-H bending CONH), 1526 (N-H bending SO_2NH), 1381 (S=O asymm. str.), 1276 (C-N str.), 1129 (S=O symm. str.), 823 (para oop), 779 (S-N str.); Mass (m/z): 376.17 ($M+H^+$); HPLC purity: 97.63%

N-(4-(N-(pyridin-2-yl)sulfamoyl)phenyl)nonanamide (SP-NON)

Cream white powder; Yield: 43.398%; UV absorption maxima:265nm; m.p. (DSC) 210.82°C; ^{1}H NMR (400 MHz, DMSO) δ 10.23 (s, 1H, amide-H), 8.00 (d, *J* = 4.5 Hz, 1H, Ar-H), 7.86 – 7.56 (m, 5H, Ar-H), 7.12 (d, *J* = 8.6 Hz, 1H, Ar-H), 6.93 – 6.58 (m, 1H, Ar-H), 2.30 (t, *J* = 7.4 Hz, 2H, CH_2), 1.65 – 1.42 (m, 2H, CH_2), 1.24 (d, *J* = 8.5 Hz, 10H), 0.83 (t, *J* = 6.8 Hz, 3H, CH_3).^{13}C NMR (500 MHz, DMSO): 171.76, 152.73, 144.14, 142.56, 139.92, 135.10, 127.67, 118.31, 113.25, 36.32, 31.10, 28.60, 28.48, 28.43, 24.81, 21.93, 13.80; IR (KBr) ν: 3331(N-H str. SO_2NH/CONH), 2922 (C-H str. ArH), 2854 (C-H str. aliphatic), 1696 (C=O str. amide), 1629 and 1459 (C=C ArH), 1592 (N-H bending CONH), 1532 (N-H bending SO_2NH), 1379 (S=O asymm. str.), 1271 (C-N str.), 1135 (S=O symm. str.), 1001 (para oop), 845 (S-N str.); Mass (m/z): 390.25 ($M+H^+$); HPLC purity: 97.44%

N-(4-(N-(pyridin-2-yl)sulfamoyl)phenyl)decanamide (SP-DEC)

Cream white powder; Yield: 40.00%; UV absorption maxima: 265nm; m.p. (DSC) 183.91°C; ^{1}H NMR (400 MHz, DMSO) δ 10.21 (s, 1H,amide-H), 8.02 (d, *J* = 4.5 Hz, 1H, Ar-H), 7.86 – 7.59 (m, 5H, Ar-H), 7.12 (d, *J* = 8.6 Hz, 1H, Ar-H), 6.98 – 6.73 (m, 1H, Ar-H), 2.31 (t, *J* = 7.4 Hz, 2H, CH_2), 1.57 (m, 2H, CH_2), 1.25 (m, 12H), 0.84 (t, *J* = 6.8 Hz, 3H, CH_3); ^{13}C NMR (500 MHz, $CDCl_3$): 172.46, 154.24, 142.46, 141.82, 141.71, 135.96, 127.76, 119.48, 115.74, 114.73, 37.76, 31.84, 29.46, 29.40, 29.29, 29.27, 25.54, 22.64, 14.08; IR (KBr) ν: 3335 (N-H str. SO_2NH/CONH), 2924 (C-H str. ArH), 2850 (C-H str. aliphatic), 1696 (C=O str. amide), 1630 and 1459 (C=C ArH), 1592 (N-H bending CONH), 1531 (N-H bending SO_2NH), 1381 (S=O asymm. str.), 1244 (C-N str.), 1135 (S=O symm. str.), 846 (para oop), 774 (S-N str.); Mass (m/z): 404.20 ($M+H^+$); HPLC purity: 97.69%

N-(4-(N-(pyridin-2-yl)sulfamoyl)phenyl)undecanamide (SP-UNDEC)

Cream white powder; Yield: 56%; UV absorption maxima: 265 nm; m.p. (DSC) 147.12 °C. ^{1}H NMR (400 MHz, DMSO) δ 10.21 (s, 1H, amide-H), 8.02 (d, *J* = 3.9 Hz, 1H, Ar-H), 7.74 (m, 5H, Ar-H), 7.12 (d, *J* = 8.5 Hz, 1H, Ar-H), 6.87 (m, 1H, Ar-H), 2.31 (t, *J* = 7.2 Hz, 2H, CH_2), 1.56 (m, 2H, CH_2), 1.23 (m, 14H), 0.83 (t, *J* = 7.2 Hz, 3H, CH_3); ^{13}C NMR (500 MHz, $CDCl_3$):

172.31, 154.07, 142.70, 141.73, 141.58, 136.00, 127.83, 119.44, 115.91, 114.68, 37.81, 31.87, 29.57, 29.51, 29.40, 29.29, 25.52, 22.66, 14.09; IR (KBr) ν: 3306 (N-H str. SO_2NH/CONH), 2918 (C-H str. ArH), 2848 (C-H str. aliphatic), 1665 (C=O str. amide), 1630 and 1463 (C=C ArH), 1595 (N-H bending CONH), 1526 (N-H bending SO_2NH), 1360 (S=O asymm. str.), 1285 (C-N str.), 1136 (S=O symm. str.), 829 (para oop), 774 (S-N str.); Mass (m/z): 418.35 ($M+H^+$); HPLC purity: 98.34%

N-(4-(N-(pyridin-2-yl)sulfamoyl)phenyl)dodecanamide (SP-DODEC)

Cream white powder; Yield: 37.00%; UV absorption maxima: 265nm; m.p. (DSC) 150.61°C.^{1}H NMR (400 MHz, $CDCl_3$) δ 8.38 (d, *J* = 5.1 Hz, 1H, Ar-H), 8.18 (b, 1H, Amide-H), 7.78 – 7.44 (m, 6H, Ar-H), 6.87 (m,1H, Ar-H), 2.40 (t, *J* = 7.2 Hz, 2H, CH_2), 1.71 (m, 2H, CH_2), 1.36 – 1.12 (m, 16H), 0.87 (t, *J* = 6.8 Hz, 3H, CH_3); ^{13}C NMR (500 MHz, $CDCl_3$): 172.26, 154.03, 142.85, 141.70, 141.48, 136.02, 127.84, 119.42, 115.96, 114.65, 37.82, 31.89, 29.63, 29.60, 29.51, 29.41, 29.32, 29.30, 25.52, 22.67, 14.10; IR (KBr) ν: 3341 (N-H str. SO_2NH/CONH), 2918 (C-H str. ArH), 2849 (C-H str. aliphatic), 1692 (C=O str. amide), 1629 and 1462 (C=C ArH), 1596 (N-H bending CONH), 1516 (N-H bending SO_2NH), 1383 (S=O asymm. str.), 1285 (C-N str.), 1131 (S=O symm. str.), 840 (para oop), 791 (S-N str.); Mass (m/z): 432.23 ($M+H^+$); HPLC purity: 99.75%

N-(4-(N-(pyridin-2-yl)sulfamoyl)phenyl)stearamide (SP-STYL)

Cream white powder; Yield: 45.54%; UV absorption maxima: 265nm. ^{1}H NMR (400 MHz, DMSO) δ 10.21 (s, 1H, amide-H), 8.02 (b, 1H, Ar-H), 7.69 – 7.81 (m, 5H, Ar-H), 7.11 – 7.13 (d, *J* = 7.5 Hz, 1H, Ar-H), 6.86 (m, 1H, Ar-H), 2.31 (b, 2H, CH_2), 1.56 (m, 2H, CH_2), 1.22 (m, 28H), 0.84 (b, 3H, CH_3). ^{13}C NMR (500 MHz, DMSO): 174.35, 151.74, 142.55, 140.67, 139.96, 135.08, 127.66,118.30, 115.48, 113.24, 39.08, 38.91, 36.32, 33.54, 31.16, 28.89, 28.61, 28.57, 28.48, 28.42, 24.80, 24.37, 21.96, 13.82; IR (KBr) ν: 3332 (N-H str. SO_2NH/CONH), 2915 (C-H str. ArH), 2848 (C-H str. aliphatic), 1697 (C=O str. amide), 1630 and 1465 (C=C ArH), 1596 (N-H bending CONH), 1526 (N-H bending SO_2NH), 1389 (S=O asymm. str.), 1291 (C-N str.), 1136 (S=O symm. str.), 1110 (para oop), 835 (S-N str.); Mass (m/z): 516.3 ($M+H^+$); HPLC purity: 96.87%

***N-(4-(N-(pyridin-2-yl)sulfamoyl)phenyl)pent-4-enamide* (SP-4-PEN)**

White powder; Yield: 76.73%; UV absorption maxima: 265nm; ^{1}H NMR (500 MHz, DMSO) δ 10.26 (s, 1H, amide-H), 8.01 – 8.02 (d, *J* = 4.7 Hz, 1H, Ar-H), 7.79 – 7.81 (m, 2H, Ar-H), 7.67 – 7.81 (m, 3H, Ar-H), 7.11 – 7.13 (d, *J* = 8.5 Hz, 1H, Ar-H), 6.85 – 6.87 (m, 1H, Ar-H), 5.79 – 5.87 (m, 1H, Alkenyl-H), 5.03 – 5.06 (m, 1H, Alkenyl-H), 4.95 – 5.06 (m, 1H, Alkenyl-H), 2.41 – 2.49 (m, 2H, CH_2), 2.30 – 2.34 (m, 2H, CH_2). ^{13}C NMR (500 MHz, DMSO): 171.03, 152.76, 142.49, 139.90, 137.27, 135.22, 127.70, 118.38, 115.80, 115.18, 113.32, 35.42, 28.72; IR (KBr) ν: 3299 (N-H str. SO_2NH/CONH), 2920 (C-H str. ArH), 2813 (C-H str. aliphatic), 1664 (C=O str. amide), 1626 and 1459 (C=C ArH), 1593 (N-H bending CONH), 1532 (N-H bending SO_2NH), 1381 (S=O asymm. str.), 1270 (C-N str.), 1130 (S=O symm. str.), 836 (para oop), 783 (S-N str.); Mass (m/z): 332.05 ($M+H^+$); HPLC purity: 99.81%

N-(4-(N-(pyridin-2-yl)sulfamoyl)phenyl)undec-10-enamide (SP-10UNDEC)

Cream white powder; Yield: 49.01%; UV absorption maxima: 265nm; m.p. (DSC) 108.84°C. ^{1}H NMR (400 MHz, DMSO) δ 10.35 (s, 1H , amide-H), 8.01 – 8.02 (d, *J* = 4.7 Hz, 1H , Ar-H), 7.67 – 7.81 (m, 5H , Ar-H), 7.11 – 7.13 (d, *J* = 8.6 Hz, 1H , Ar-H), 6.85 – 6.88 (m, *J* = 6.2 Hz, 1H, Ar-H), 5.72-5.82 (m, 1H), 4.90 – 5.00 (m, 2H, CH_2), 3.56 – 3.63 (m, 1H), 3.09 – 3.14 (m, 1H), 2.34 (t, *J* = 7.4 Hz, 2H), 1.25 – 2.01 (m, 12H). ^{13}C NMR (500 MHz, DMSO):171.81, 152.75, 142.62, 139.84, 138.68, 135.08, 127.63, 118.31, 115.83, 114.49, 113.27, 36.29, 33.03, 28.59, 28.45, 28.33, 28.10, 24.82; IR (KBr) ν: 3323 (N-H str. SO_2NH/CONH), 2924 (C-H str. ArH), 2853 (C-H str. aliphatic), 1691 (C=O str. amide), 1629 and 1460 (C=C ArH), 1591 (N-H bending CONH), 1528 (N-H bending SO_2NH), 1384 (S=O asymm. str.), 1271 (C-N str.), 1130 (S=O symm. str.), 847 (para oop), 774 (S-N str.); Mass (m/z): 416.6 ($M+H^+$); HPLC purity: 98.69%

***(E)-N-(4-(N-(pyridin-2-yl)sulfamoyl)phenyl)octadec-9-enamide* (SP-OLE)**

Yellowish powder; Yield: 27%; UV absorption maxima: 265nm; ^{1}H NMR (400 MHz, DMSO) δ 10.21 (s, 1H, amide-H), 8.01-8.02 (d, *J* = 4.3 Hz, 1H, Ar-H), 7.67 – 7.81 (m, 5H, Ar-H), 7.11– 7.13 (d, J = 8.6 Hz, 1H, Ar-H), 6.85 – 6.88 (m, 1H, Ar-H), 5.27 – 5.64 (m, 2H, Alkenyl-H), 2.29 – 2.32 (t, *J* = 7.4 Hz, 2H, CH_2), 1.96 – 1.97 (d, *J* = 5.1 Hz, 4H), 1.54 – 1.58 (m, 2H, CH_2), 1.21– 1.26 (m, 20H), 0.80 – 0.84 (t, *J* = 6.8 Hz, 3H, CH_3). ^{13}C NMR (500 MHz, DMSO):171.70, 152.75, 143.89, 142.57, 135.09, 129.51, 129.47, 118.29, 115.92, 113.23, 36.31, 31.14, 28.96, 28.55, 28.52, 28.48, 28.46, 28.36, 26.44, 24.80, 21.95, 13.79; IR (KBr) ν: 3336 (N-H str. SO_2NH/CONH), 2920 (C-H str. ArH), 2851 (C-H str. aliphatic), 1668 (C=O str. amide), 1629 and 1460 (C=C ArH), 1597 (N-H bending CONH), 1525 (N-H bending SO_2NH), 1383 (S=O asymm. str.), 1280 (C-N str.), 1136 (S=O symm. str.), 830 (para oop), 795 (S-N str.); Mass (m/z): 514.4 ($M+H^+$); HPLC purity: 95.16%

4.2 Characterization of N-substituted amino acid-based prodrugs of SP

***tert-butyl (2-oxo-2-((4-(N-(pyridin-2-yl)sulfamoyl)phenyl)amino)ethyl)carbamate* (SP-GLY)**

White powder; Yield: 82%; UV absorption maxima: 265nm; 1H NMR (500 MHz, DMSO) δ 11.79 (s, 1H, amide-H), 10.26 (s, 1H, amide-H), 8.00-8.01 (d, *J* = 4.6 Hz, 1H, Ar-H), 7.80-7.82 (m, 2H, Ar-H), 7.67 – 7.71 (m, 3H, Ar-H), 7.11 – 7.13 (d, *J* = 8.5 Hz, 1H, Ar-H), 7.04 – 7.07 (t, *J* = 5.4 Hz, 1H, NH), 6.84 – 6.87 (m, 1H, Ar-H), 3.72 – 3.73 (α 2H), 1.30 – 1.37 (m, 9H, Boc-H). ^{13}C NMR (500 MHz, DMSO):168.78, 152.83, 142.17, 139.97, 135.47, 127.75, 118.46, 115.73, 113.41, 78.02, 43.77, 28.09; IR (KBr) ν: 3387 (N-H str. SO_2NH/CONH), 2925 (C-H str. ArH), 2852 (C-H str. aliphatic), 1678 (C=O str. amide), 1630 and 1464 (C=C ArH), 1594 (N-H bending CONH), 1551 (N-H bending SO_2NH), 1367 (S=O asymm. str.), 1315 (C-N str.), 1135 (S=O symm. str.), 833 (para oop), 771 (S-N str.), 1243 (C-O str. carbamate); Mass (m/z): 407.11 ($M+H^+$); HPLC purity: 99.63%

***tert-butyl (S)-(1-oxo-1-((4-(N-(pyridin-2-yl)sulfamoyl)phenyl)amino)propan-2-yl)carbamate* (SP-LALA)**

White powder; Yield: 50%; UV absorption maxima: 265nm; ^{1}H NMR (500 MHz, DMSO) δ 11.60 (s, 1H, amide-H), 10.26 (s, 1H, amide-H), 8.00 – 8.01 (d, *J* = 4.6 Hz, 1H, Ar-H), 7.81 – 7.82 (m, 2H, Ar-H), 7.66 – 7.74 (m, 3H, Ar-H), 7.10 – 7.12 (b, 2H, Ar-H & NH), 6.84 – 6.86 (m, 1H, Ar-H), 4.08 – 4.11(α H), 1.23 – 1.36 [m, 12H (9H, Boc-H & 3H, CH_3)]. ^{13}C NMR (500 MHz, DMSO):171.44, 152.84, 142.33, 135.47, 127.72, 118.55, 115.74, 113.34, 50.45, 28.09, 17.63; IR (KBr) ν: 3320 (N-H str. SO_2NH/CONH), 2923 (C-H str. ArH), 2852 (C-H str. aliphatic), 1711 (C=O str. amide), 1630 and 1461 (C=C ArH), 1588 (N-H bending CONH), 1525 (N-H bending SO_2NH), 1383 (S=O asymm. str.), 1285 (C-N str.), 1130 (S=O symm. str.), 840 (para oop), 777 (S-N str.), 1267 (C-O str. carbamate); Mass (m/z): 421.12 ($M+H^+$); HPLC purity: 98.09%

***tert-butyl (S)-(4-methyl-1-oxo-1-((4-(N-(pyridin-2-yl)sulfamoyl)phenyl)amino)pentan-2-yl)carbamate* (SP-LLEU)**

White powder; Yield: 68%; UV absorption maxima: 265 nm; ^{1}H NMR (500 MHz, DMSO) δ 11.76 (s, 1H, amide-H), 10.28 (s, 1H, amide-H), 8.00 – 8.01 (d, *J* = 4.5 Hz, 1H, Ar-H), 7.81 – 7.82 (m, 2H, Ar-H), 7.67 – 7.75 (m, 3H, Ar-H), 7.11 – 7.13 (d, J = 8.6 Hz, 1H, Ar-H), 7.05 – 7.07 (d, *J* = 7.7 Hz, 1H, NH), 6.84 – 6.87 (m, 1H, Ar-H), 4.01 – 4.11 (α H), 1.48 – 1.64 (m, β 2H), 1.33 – 1.42 (m, 9H, Boc-H), 1.21 – 1.22 (m, γ H), 0.84 – 0.88 (m, 6H). ^{13}C NMR (500 MHz, DMSO):172.37, 155.37, 152.78, 142.28, 139.91, 135.53, 127.70, 118.64, 115.75, 113.32, 77.96, 59.63, 53.52, 28.07, 24.22, 22.80, 21.38; IR (KBr) ν: 3355 (N-H str. SO_2NH/CONH), 2923 (C-H str. ArH), 2851 (C-H str. aliphatic), 1702 (C=O str. amide), 1631 and 1462 (C=C ArH), 1588 (N-H bending CONH), 1518 (N-H bending SO_2NH), 1386 (S=O asymm. str.), 1269 (C-N str.), 1131 (S=O symm. str.), 847 (para oop), 771 (S-N str.), 1248 (C-O str. carbamate); Mass (m/z): 463.17 ($M+H^+$); HPLC purity: 99.68%

***tert-butyl (S)-2-((4-(N-(pyridin-2-yl)sulfamoyl)phenyl)carbamoyl)pyrrolidine-1-carboxylate* (SP-LPRO)**

White powder; Yield: 89%; UV absorption maxima: 265 nm; ^{1}H NMR (500 MHz, DMSO) δ 11.60 (s, 1H, amide-H), 10.31 (s, 1H, amide-H), 8.00 – 8.01 (d, *J* = 4.8 Hz, 1H, Ar-H), 7.80 – 7.82 (m, 2H, Ar-H), 7.67 – 7.73 (m, 3H, Ar-H), 7.10 – 7.13 (d, *J* = 8.4 Hz, 1H, Ar-H), 6.84 – 6.87 (m, 1H, Ar-H), 4.17 – 4.25 (m, αH Proline), 3.40-3.41 (m, 2H Proline), 1.76-2.21 (m, 4H Proline), 1.23-1.37 (m, 9H, Boc-H). ^{13}C NMR (500 MHz, DMSO):172.04, 153.52, 152.98, 142.29, 139.98, 135.47, 127.74, 118.57, 113.43, 78.69, 60.33, 46.64, 30.01, 28.05, 23.26; IR (KBr) ν: 3293 (N-H str. SO_2NH/CONH), 2918 (C-H str. ArH), 2850 (C-H str. aliphatic), 1707 (C=O str. amide), 1627 and 1462 (C=C ArH), 1589 (N-H bending CONH), 1518 (N-H bending SO_2NH), 1379 (S=O asymm. str.), 1269 (C-N str.), 1248 (C-O str. carbamate), 1126 (S=O symm. str.), 847 (para oop), 772 (S-N str.); Mass (m/z): 447.13 ($M+H^+$); HPLC purity: 99.19%

4.3 Fabrication and characterization of self-assembled nanostructures

The self-assembled nanostructures of synthesized prodrugs were developed by kinetic trapping, also known as nanoprecipitation method. Based on the morphology, stability, and hydrodynamic diameters of self-assembled particles, SP-LLEU was found to form stable nanostructures of optimum size. Particle size, PDI and zeta potential of SP-LLEU nanoparticles were found to be 635 nm, 0.070 and -24.5 mV respectively. The size distribution, zeta potential and microscopic image of SP-LLEU nanoparticles have been depicted in Figure 4 A- C respectively.

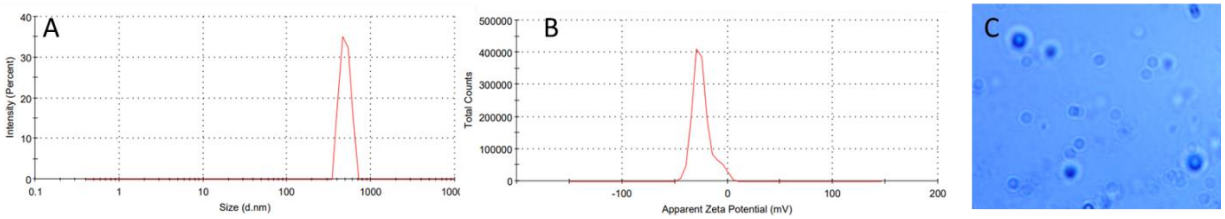

Figure 4: Size distribution, zeta potential and microscopic image of SP-LLEU nanoparticle (A-C)

4.4 Analytical method development and validation

An efficient reverse phase HPLC method for SP-LLEU prodrug was developed and validated as per ICH Q2 (R1) guidelines. The retention time of prodrug was found to 4.201 ± 0.005 min, and the method was found to be linear in the concentration range of 2 to 10 µg/mL. Recovery of the individual values was in range of 96.15-101.92%, with relative standard deviation of less than 2%. HPLC chromatogram and linearity plot have been depicted in Figure 5. Various chromatographic parameters are summarized in Table 1.

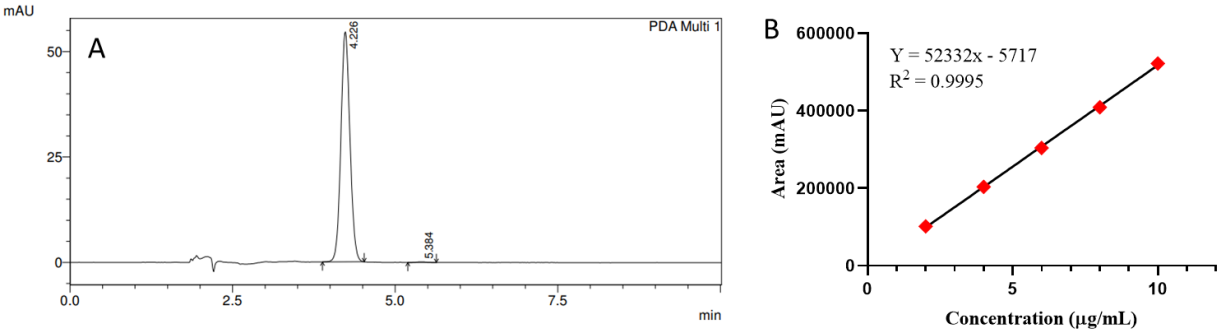

Figure 5: HPLC chromatogram (A) and linearity plot (B) of SP-LLEU

Table 1: Chromatographic data of SP-LLEU

Parameter	**Average ± SD**
Retention time (R_t, min)	4.201 ± 0.005
Run-time (min)	10
Retention factor (k)	0.443 ± 0.001
Theoretical plate (N)	3892.086 ± 67.479
Tailing factor (T)	1.733 ± 0.014
Peak area (A)	522266.200 ± 4329.009
Organic solvent per run (mL)	6.5 mL

4.5. Physicochemical characterization of prodrugs

Equilibrium solubility and partition coefficient of the SP-LLEU prodrug as well as of SP was determined by shake-flask experiments. The prodrug has been found to possess lower aqueous solubility as compared to that of SP. This can be attributed to incorporation of BoC protected amino acid moiety that gives a lipophilic character to the molecule. As compared to SP, prodrug exhibited a remarkable increase in solubility in *n*-octanol. Similarly, prodrug exhibited high log P value as compared to SP, which is also in agreement with results of solubility studies. The solubility profiles and partition coefficients of both SP and SP-LLEU prodrug have been summarized in Table 2.

Table 2: Thermodynamic equilibrium solubility and log P of SP and its prodrug

Drug	**Thermodynamic solubility studies (mg/L)**		**Log $P_{oct/water}$**
	n-Octanol	**Water**	
SP	213.56 ± 12.45	221.27 ± 5.59	0.0385 ± 0.0012
SP-LLEU prodrug	332.16 ± 7.24	33.75 ± 5.67	0.993 ± 0.004

4.5. *In vitro* cytotoxicity studies

In vitro cytotoxicity study demonstrated the comparable safety of prodrug to that of SP. The cell viability was found to be more than 50% at a concentration of 500 µM. These observations in the MTT assay indicate that the synthesized prodrug is safer and biocompatible in nature upto concentration of ~ 65 µg/mL.

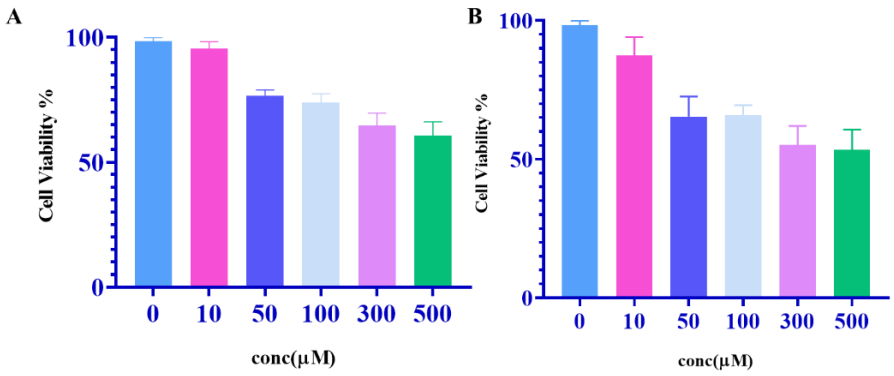

Figure 6: Percentage cell viability of SP (A) and SP-LLEU prodrug (B)

4.6. *In vivo* antiarthritic activity

Intra-articular administration of self-assembled prodrug nanostructures successfully mitigated the inflammation, as demonstrated by normalized levels of inflammatory mediators, hematological parameters, and other biochemical parameters. High dose group was found to be more effective in ameliorating symptoms of inflammatory arthritis as compared to low dose group, which in turn was more effective than SP suspension. This demonstrates the effectiveness of self-assembled nanostructures over other conventional formulations, which is attributed to controlled release of drugs from this smart delivery systems. The summarizes results of pharmacological evaluation have been shown in Table 3-5 and Figure 7.

Table 3: Effect of SP and prodrug nanoparticle on haematological parameters in CFA-induced arthritis

Groups	**Hb (g/dL)**	**RBC (10^6/µL)**	**WBC (10^3/µL)**	**Platelet (10^3/µL)**	**Hematocrit (%) HCT**
Control Group	14.61 ± 1.53	8.50 ± 0.85	7.56 ± 1.34	846.24 ± 24.54	45.32 ± 2.65
CFA	8.93 ± 0.85	5.16 ± 0.67	12.38 ± 0.76	1283.76 ± 34.76	24.24 ± 1.65
SPD suspension	11.58 ± 1.24	6.15 ± 1.12	10.38 ± 1.47	1091.17 ± 76.24	36.92 ± 1.24
SPD-LLEU suspension	14.2 ± 0.76	7.23 ± 0.37	9.29 ± 0.46	930.55 ± 29.35	39.73 ± 1.14
SPD-LLEU self-assembly low dose	16.4 ± 2.17	8.04 ± 1.27	7.76 ± 1.17	898.64 ± 56.56	41.33 ± 1.17
SPD-LLEU self-assembly high dose	17.7 ± 1.64	8.35 ± 0.78	7.06 ± 0.34	865.34 ± 34.57	44.34 ± 0.93

Table 4: Effect of SP and prodrug nanoparticle on serum parameters in CFA-induced arthritis

Groups	RF (IU/mL)	C-reactive protein (µg/mL)	Total protein (g/dL)	AST (IU/L)	ALT (IU/L)	ALP (IU/L)
Control Group	-	425.23 ± 24.68	7.83 ± 0.59	154.02 24.58	70.43 ± 12.24	70.66 ± 16.25
CFA	8.84 ± 1.17	1138.48 ± 86.24	4.06 ± 0.65	348.75 ± 56.54	155.05 ± 16.24	432.81 ± 56.24
SPD suspension	6.64 ± 1.25	890.45 ± 37.49	5.77 ± 0.47	268.14 ± 22.95	118.42 ± 16.27	250.26 ± 24.25
SPD-LLEU suspension	6.64 ± 0.97	745.56 ± 29.82	6.07 ± 0.84	271.66 ± 29.98	90.41 ± 10.54	225.07 ± 16.20
SPD-LLEU self-assembly low dose	5.23 ± 2.08	658.17 ± 28.84	6.50 ± 0.79	213.04 ± 55.49	82.14 ± 15.67	134.21 ± 11.28
SPD-LLEU self-assembly high dose	4.05 ± 1.39	563.25 ± 63.37	7.76 ± 1.24	183.61 ± 39.56	75.65 ± 8.25	85.21 ± 8.15

Table 5: Effect of SP and prodrug nanoparticle on the production of inflammatory cytokines in CFA rats

Groups	IL6 (pg/mL)	TNF-α (pg/mL)
Control Group	74.62 ± 5.16	2425.23 ± 32.56
CFA	568.54 ± 11.17	21956.48 ± 98.51
SPD suspension	306.04 ± 16.25	12489.76 ± 77.54
SPD-LLEU suspension	206.64 ± 17.97	12254.29 ± 39.65
SPD-LLEU self-assembly low dose	135.23 ± 15.08	6651.17 ± 20.59
SPD-LLEU self-assembly high dose	94.05 ± 6.39	4657.68 ± 32.59

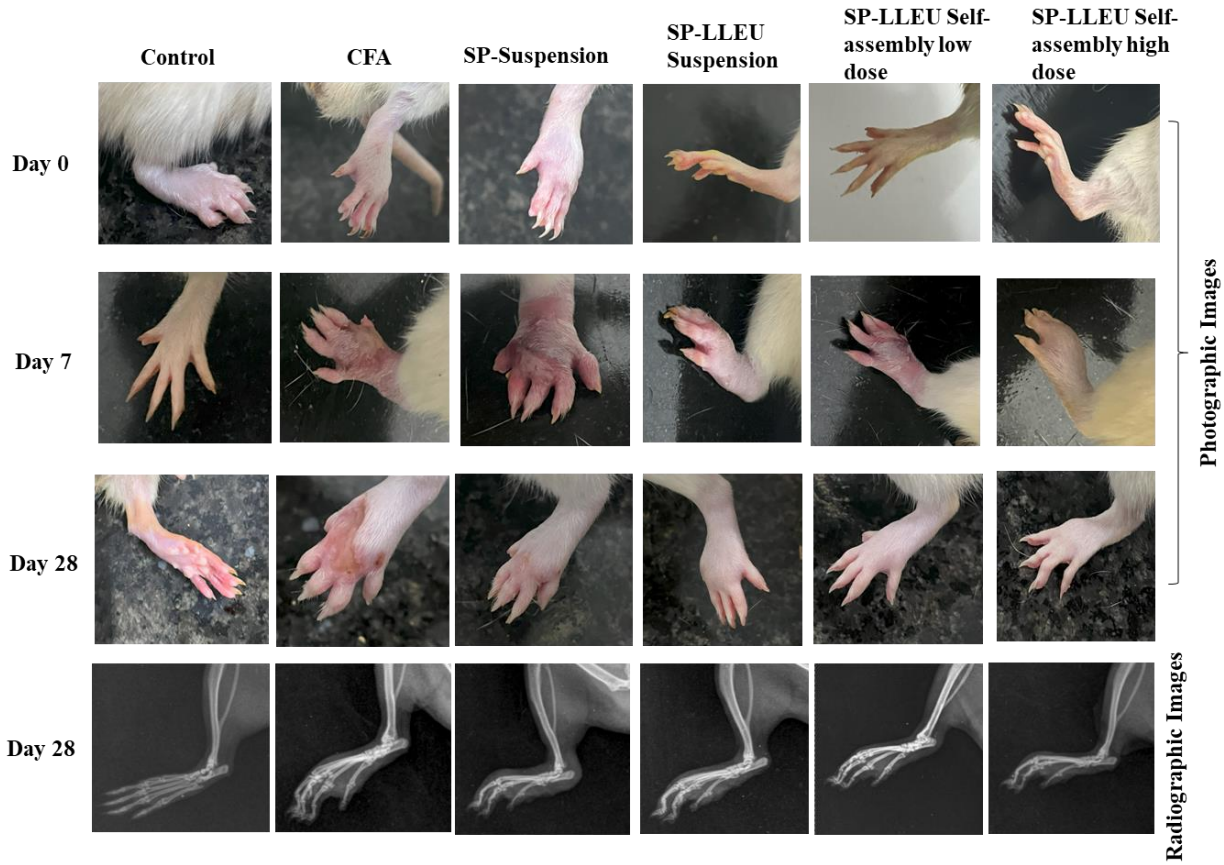

Figure 7: Digital images and X-ray images of hind paw of normal control, arthritic control, SP suspension, SP-LLEU suspension, SP-LLEU self-assembly low dose, and SP-LLEU self-assembly high dose

5. Statistical Analysis

The data were analyzed with Microsoft Excel 2021 and expressed as mean ± SD.

6. Impact of the research in the advancement of knowledge or benefit to mankind:

A single intra-articular injection of self-assembling supramolecular nanostructures of SP prodrug successfully mitigated the inflammation in adjuvant-induced arthritis. The encouraging results obtained in the current preclinical studies further inspires to evaluate the developed delivery system in human subjects suffering from RA. The developed technology is expected to provide an economical, and patient friendly therapeutic approach for the management of arthritis.

7. Literature References:

1. Smolen, J.S., et al., *Treating rheumatoid arthritis to target: 2014 update of the recommendations of an international task force.* Annals of the rheumatic diseases, 2016. **75**(1): p. 3-15.

2. Burmester, G.R. and J.E. Pope, *Novel treatment strategies in rheumatoid arthritis.* The Lancet, 2017. **389**(10086): p. 2338-2348.

3. Kesharwani, D., et al., *Rheumatiod Arthritis: An Updated Overview of Latest Therapy and Drug Delivery.* J Pharmacopuncture, 2019. **22**(4): p. 210-224.

4. Kapoor, B., et al., *Fail-safe nano-formulation of prodrug of sulfapyridine: Preparation and evaluation for treatment of rheumatoid arthritis.* Materials Science and Engineering: C, 2021. **118**: p. 111332.

5. Patra, J.K., et al., *Nano based drug delivery systems: recent developments and future prospects.* Journal of Nanobiotechnology, 2018. **16**(1): p. 71.

6. Khan, F., et al., *Synthesis, classification and properties of hydrogels: their applications in drug delivery and agriculture.* Journal of Materials Chemistry B, 2022. **10**(2): p. 170-203.

7. Pattni, B.S., V.V. Chupin, and V.P. Torchilin, *New Developments in Liposomal Drug Delivery.* Chemical Reviews, 2015. **115**(19): p. 10938-10966.

8. Medina, S.H. and M.E.H. El-Sayed, *Dendrimers as Carriers for Delivery of Chemotherapeutic Agents.* Chemical Reviews, 2009. **109**(7): p. 3141-3157.

9. Guterres, S.S., M.P. Alves, and A.R. Pohlmann, *Polymeric nanoparticles, nanospheres and nanocapsules, for cutaneous applications.* Drug Target Insights, 2007. **2**: p. 147-57.

10. Navya, P.N., et al., *Current trends and challenges in cancer management and therapy using designer nanomaterials.* Nano Convergence, 2019. **6**(1): p. 23.

11. Dong, X., et al., *Stimulus-responsive self-assembled prodrugs in cancer therapy.* Chem Sci, 2022. **13**(15): p. 4239-4269.

12. Cheetham, A.G., et al., *Self-assembling prodrugs.* Chemical Society reviews, 2017. **46**(21): p. 6638-6663.

13. Rani, P., et al., *Nanoscale self-assembling prodrugs of sulfapyridine for treatment of arthritis: Harnessing the dual approach.* Medical Hypotheses, 2022. **165**: p. 110896.

14. Liu, G., et al., *Stimulus-Responsive Nanomedicines for Disease Diagnosis and Treatment.* Int J Mol Sci, 2020. **21**(17).

15. Liu, X.H., et al., *Recent advances in enzyme-related biomaterials for arthritis treatment.* Front Chem, 2022. **10**: p. 988051.

16. Wang, X., et al., *The Role of Reactive Oxygen Species in the Rheumatoid Arthritis-Associated Synovial Microenvironment.* Antioxidants (Basel), 2022. **11**(6).

17. Zhang, M., et al., *Advanced application of stimuli-responsive drug delivery system for inflammatory arthritis treatment.* Mater Today Bio, 2022. **14**: p. 100223.

18. Joshi, N., et al., *Towards an arthritis flare-responsive drug delivery system.* Nature Communications, 2018. **9**(1): p. 1275.

Sign of the Applicant

Pooja Rani